Autophage Engines: Towards a Throttleable Solid Motor

Vitaly Yemets[*]
Oles Honchar Dnipro National University, 72 Gagarin Avenue, Dnipro, 49010, Ukraine

Patrick Harkness[†]
University of Glasgow, University Avenue, Glasgow, G12 8QQ, United Kingdom

Mykola Dron'[‡], Anatoly Pashkov[§]
Oles Honchar Dnipro National University, 72 Gagarin Avenue, Dnipro, 49010, Ukraine

Kevin Worrall[**], Michael Middleton[††]
University of Glasgow, University Avenue, Glasgow, G12 8QQ, United Kingdom

This paper describes the instrumented test-firing of a rocket which seeks to combine the throttleability of a liquid-fueled engine with the simplicity of a solid motor. The concept is that a differentiated fuel and oxidizer rod is forced into a vaporization unit where its constituents transition into separate propellant gases, which are then mixed in a combustion chamber. The vaporization unit is heated by the combustion and the throttle setting is adjusted by changing the force used to drive the solid propellant rod into the vaporizer, which naturally influences the propellant feed rate. In experiments using a solid propellant rod consisting of polypropylene fuel and a 1:1.5 mixture of NH_4ClO_4 and NH_4NO_3 oxidizer, we have sustained operations for around sixty seconds. During testing, using propellant feed forces of between 250 N and 900 N, we have achieved propellant feed rates of between 100 mm/min and 300 mm/min, which are in turn correlated to chamber pressures of between approximately 300 kPa and 700 kPa. These correlated cycles of control input (the feed force), throttle response (the propellant feed rate) and implied thrust (the chamber pressure) demonstrate, for the first time, a simple solid rocket that can be throttled in real time.

---

[*] Professor, Physical and Technical Faculty.
[†] Senior Lecturer, School of Engineering.
[‡] Professor, Physical and Technical Faculty.
[§] Senior Researcher, Institute of Power Engineering.
[**] Research Associate, School of Engineering.
[††] MSc Student, School of Engineering.

I. Introduction

LIQUID fueled engines can be throttled and even restarted by pumping fuel and oxidizer into the combustion chamber as desired, but their turbo-pump feed systems, injection heads, cooling channels and slosh preventers make them expensive. Pressure-feeding can reduce the cost, but adds more mass, while hypergolic liquid propellants are toxic and more dangerous to handle than their solid counterparts. Finally, pressurized vessels for liquids are sometimes forbidden on small spacecraft in order to reduce launch risks and facilitate overall compliance. [1]

Solid motors, on the other hand, can produce a desired impulse profile by shaping the propellant such that the flame front progresses in a predetermined pattern, but it is not generally possible to throttle the motor on demand. [2]

We seek a solution which combines the comparative simplicity in handling of the solid motor with the throttleability of the liquid engine, and propose that this could be delivered by an autophage motor.

Our testbed uses propellant rods in which the fuel and oxidizer are not mixed but are rather, as shown in Fig. 1, constructed with a polypropylene fuel cylinder enclosing an ammonium perchlorate/nitrate oxidizer. This means that the propellant rod can be fed into a conical vaporizer (which is heated from the combustion chamber) without the components mixing, using an external ram powered by an inert gas. When any part of the rod reaches the hot surface it vaporizes and passes through holes in the inner part of the vaporizer itself. The holes near the rim of the cone face against the outer part of the rod, and so accept predominantly gaseous fuel, while those near the apex face against the center of the rod and so accept predominately gaseous oxidizer. A system of channels on the outer surface of the vaporizer cone transport these gases, separately, to an injector ring, where they enter the combustion chamber through sixteen circumferential ports. Combustion then takes place and the exhaust gases exit through the nozzle, which has a sliding graphite throat that can be positioned (via a push-rod) to vary the throat area without stopping the engine.

The injection ports are covered by tantalum flap valves which prevent the back-passage of the products of combustion should the chamber pressure exceed the fuel feed pressure, and there are further access points for instrumentation in the chamber wall. Finally, the testbed incorporates an additional gas manifold which can provide propane, oxygen, and nitrogen from external storage tanks. These pilot gases can be ignited by a spark plug and are used to preheat the engine until the vaporization and combustion of the solid propellant has become self-sustaining. Pure nitrogen can also be supplied to extinguish and purge the engine, if required.

It is envisaged that, in future development, the propellant feeding ram will be replaced by a self-contained mechanism and the preheat function will be achieved by an electrical element rather than external pilot gases.

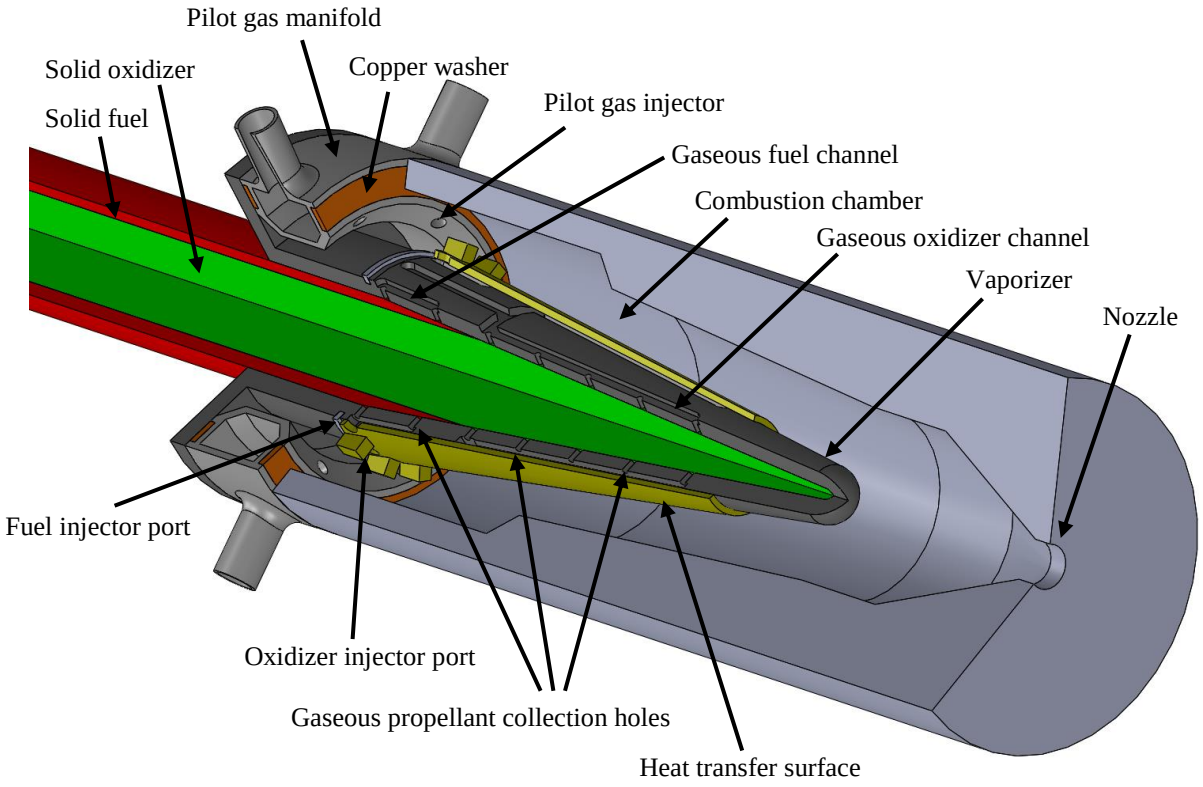

Fig. 1 A cutaway drawing of the engine. The flap valves over the injection ports are omitted.

Autophage motor concepts appear sporadically in the literature. Early patents dating from the 1930s exist [3], with other patents through the 1960's [4], 1970's [5], and 1980's [6]. To our knowledge, none of these patents detail experimental test firings, or provide concrete evidence that the devices described proved feasible. Finally, after the late 1980s, there appears to be little further discussion of autophage concepts by other authors.

This is not to say that there is no interest in throttling solid motors, but the competing schemes put forward have been complex. For example, controllable lasers [7], controllable variations in chamber pressure [8], and controllable applied electric current [9], combined with specialist propellants, have been suggested to influence combustion rates.

Given the elegance of the autophage concept, therefore, this discontinued development is something of a mystery. There has obviously been a great deal of effort expended by various parties over many decades, but there is no evidence of any working system being developed, nor is there any record of publications setting out why it was not achieved. However, the very recent work of Yemets [10, 11, 12], which records the first firing of the autophage testbed, indicates that the high pressure inside the combustion chamber may make it difficult to feed the propellant into the vaporizer.

This current study builds on that initial firing and, for the first time, presents instrumental data collected during the burn itself. We trust that this will support future development of the autophage concept.

II. Experimental Campaign

A. The facilities

The experiments were conducted in the laboratories of the Dnipro National University, using some instrumentation provided by the University of Glasgow. The facilities consist of a firing room with a gas-tight door and a separate viewing window, through which the operators can observe the engine testbed from the adjoining operations room.

The testbed is mounted such that the engine fires in an inverted manner, with the exhaust plume directed into a ventilation system mounted in the ceiling. The testbed instrumentation includes a linear position sensor to monitor consumption of the propellant rod, a force transducer to measure the force being applied to the propellant rod by the external ram, a tungsten-rhenium thermocouple mounted at the combustion chamber wall, and a pressure tap at the same location which leads to both electronic and mechanical pressure gauges. Data from these instruments is fed back through the services channel to be logged in the operations room.

One additional chamber pressure gauge and two voltmeters, linked in parallel to the thermocouple and the linear position sensor, are displayed close to engine such that they are included in video recordings of each burn. This allows the team to match features in the dataset to the physical events, such as ignition and nozzle exchanges, which are captured in the video record.

B. Preparations for each firing

Firstly, the testbed is entirely disassembled, each component is cleaned and prepared, and the condition and free operation of the tantalum flap valves is checked. Copper washers, used to seal the combustion chamber against the injector manifold, are annealed to help ensure a tight fit after reassembly. This fit is checked by pressurizing the chamber from the nitrogen supply and searching for leaks using soapy water.

Next, a propellant rod is prepared from a 20mm diameter polypropylene pipe (wall thickness 1-1.5mm), to which ammonium perchlorate and ammonium nitrate powder is added in a ratio of 1:1.5 by mass. Only a few grams of oxidizer is added at a time, and after each addition the operators leave the room and the powder is rammed using the argon gas supply. Around forty cycles are required to prepare the 120-150g of oxidizer used for each firing.

Finally, the sensors are calibrated and the rig is assembled, as shown in Fig. 2. Smooth movement of the nozzle throat exchange mechanism is confirmed, the function of the pilot gas valves and spark plug is checked, and when all is complete the operators leave the firing room and move to the operations room in Fig. 3, sealing the gas-tight door behind them.

C. Firing positions

The test director takes up position at the main desk in Fig. 3, which offers a view of the engine through the window. The director has a desktop display of the pressure being applied to the external ram, and a line of sight to a gauge displaying chamber pressure and a mirror showing a rear view of the test stand. From here, the director can adjust the ram pressure (the argon is stored to the left of the desk) and also operate a spark plug inside the combustion chamber.

The first assistant stands in an alcove just to the left of the window, but is still able to observe the engine. This assistant can operate three valves near ground level, which supply propane, oxygen, and nitrogen pilot gases, and also reach a lever just above the window. The lever is connected to the nozzle exchange pushrod, which can slide the graphite throat assembly across the chamber outlet to vary the throat area.

Finally, the second assistant sits at another desk to the right of the window. This assistant cannot see the engine, but has a live video feed on the shelf above. The second assistant is responsible for recording the video and logging the instrument data which, as with the gases and high-tension cables, are passed through an opening from the firing room. The second assistant also operates the ventilation system using a panel mounted high on the right-hand wall.

D. Firing procedure

To conduct a firing, the following steps take place:

1. The second assistant begins recording video and logging data. Some data is also displayed in real-time.
2. The director applies argon pressure to the external ram, forcing the propellant rod hard against the vaporizer.
3. The first assistant turns on the propane, oxygen, and nitrogen pilot gases. The nitrogen will limit the temperature.
4. The director operates the spark plug until ignition occurs. A yellow propane flame is seen.
5. After some tens of seconds, the second assistant reports movement of the propellant rod as vaporization begins.
6. After some further tens of seconds, blue highlights are seen in the flame. This indicates propellant combustion.
7. At the director's command, the pilot gases are turned off and the nozzle is constricted by the first assistant.
8. The director significantly reduces the argon pressure applied to the external ram.
9. The engine is now self-sustaining. Throttling, via argon pressure adjustment, may be attempted by the director.
10. The test ends due to fuel starvation or, sometimes, another failure mechanism.
11. The first assistant applies nitrogen to purge the engine, and then all the gases are turned off.
12. The ventilation system is allowed to run for 30 minutes before the door to the firing room is reopened.

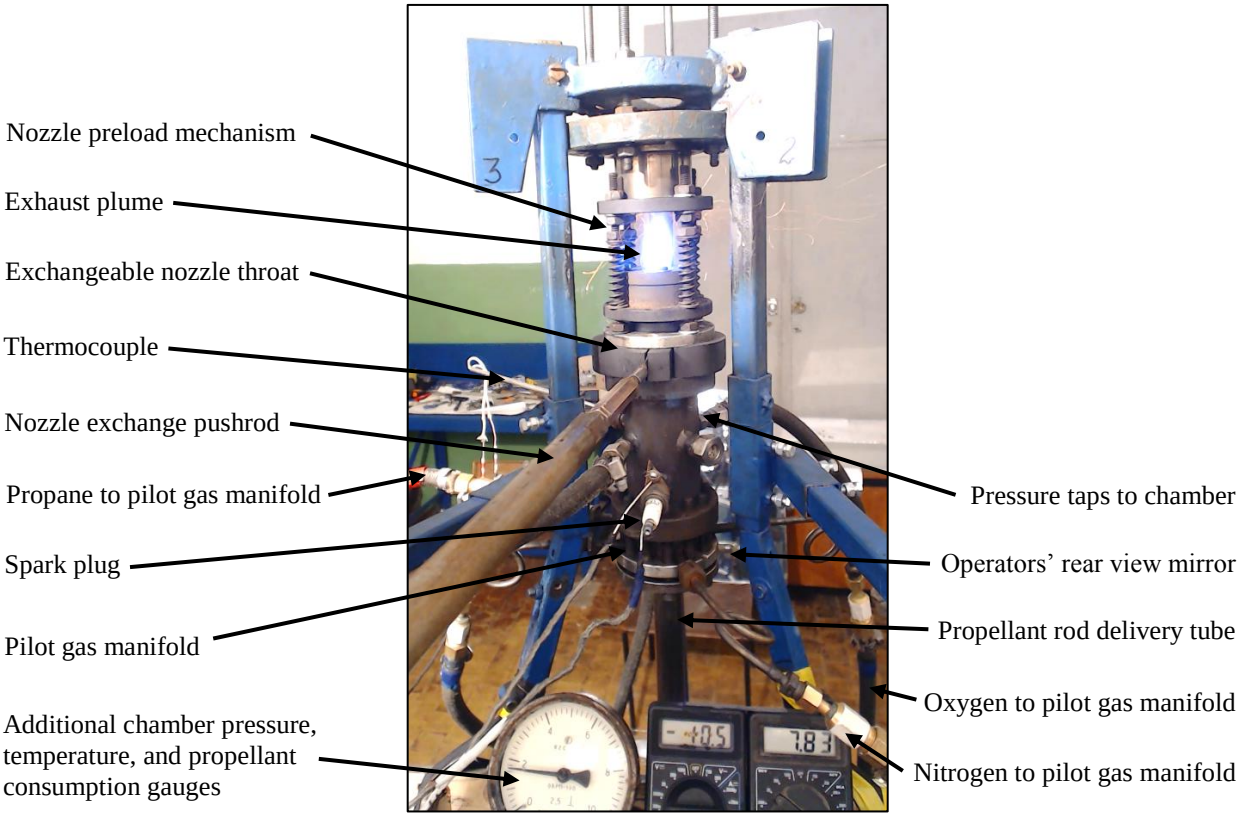

Fig. 2 The experimental rig firing, in a still taken from the video record.

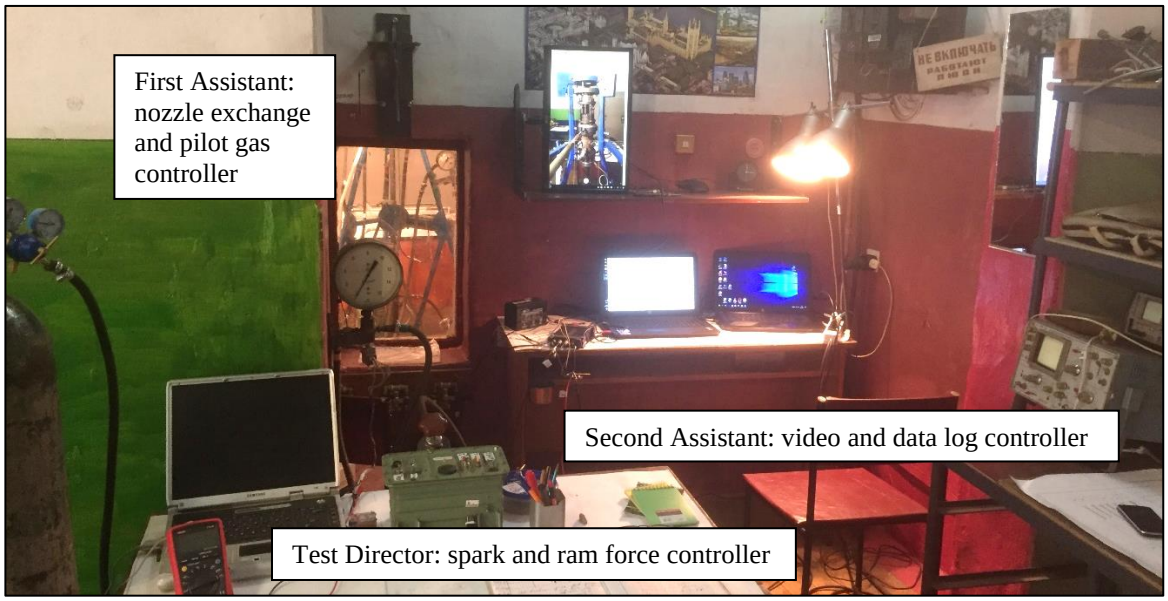

Fig. 3 The operations room, looking towards the firing room.

E. Propellant and combustion

The development team selected the propellant mixture (polypropylene fuel and a 1:1.5 mixture of ammonium perchlorate and ammonium nitrate oxidizer) after considering the fuels and oxidizers presented in Tab. 1. In this table, we consider 'free' oxygen to be the difference between the total oxygen contained in the oxidizer and the oxygen necessary to react with hydrogen present within the oxidizer itself, excluding that part of the hydrogen which will form a bond with chlorine instead.

Tab. 1 Some characteristics of fuels and oxidizers [13, 14, 15].

Propellant component	Role	Chemical formula	Enthalpy of formation (kJ/kg)	Free oxygen (g/kg)	Tensile strength (MPa)	Specific mass (g/cm^3)
Polypropylene (PP)	Fuel	$(C_3H_6)_n$	-2100…-1900	-	32	0.90…0.92
High-Pressure Polyethylene (PE)	Fuel	$(C_2H_4)_n$	-2100…-1900	-	12…16	0.92…0.93
Ammonium perchlorate (AP)	Oxidizer	NH_4ClO_4	-2513	277	powder	1.7
Ammonium nitrate (AN)	Oxidizer	NH_4NO_3	-4571	80	powder	1.4

As PP and PE have similar characteristics, there is little difference between them in firing. However, the greater mechanical strength of PP makes it more suitable for the thin casing of the propellant rod. Low-Pressure Polyethylene is as strong as PP, but has not yet been tested.

AP is superior to AN in terms of enthalpy of formation, the amount of free oxygen which can be liberated, and specific mass. However, our attempts to use pure AP have been unsuccessful, often causing burn damage to the engine. Examination has shown that the burning generally takes place inside the vaporizer and under the heat transfer surface, and on the tips of oxidizer flap valves. Specifically, the burning takes place in regions without fuel contact, and so the damage is not caused by the combustion of the propellant. The reason is likely a reaction of the hot metal with the decomposed oxidizer itself.

Therefore, to protect the structure, we have applied a zirconium oxide coating to the vaporizer and discovered, experimentally, that adding some proportion of AN to the pure AP oxidizer lessens the undesired effects. An AP:AN ratio of 1:1 still results in damage, but ratios of 1:1.5 and 1:2 generally do not. However, combustion of solid propellant at a ratio of 1:2 is so slow that the chamber pressure reaches no more than 400 kPa, which is unacceptably low for propulsion purposes. The intermediate ratio of 1:1.5 produces chamber pressures of up to 800 kPa and, given that the engine is not damaged by its use, this mixture has been chosen for our research.

An examination of Tab. 2 illustrates why this increase in relative AN content reduces the damage to the engine. Increased fractions of AN reduce the temperature, the amount of chlorine, and the amount of free oxygen in the propellant mixture, which in turn lessens the impact on the structural components. In this table, combustion products are calculated using the method of equilibrium constants, considering thermal decompositions of H_2O, CO_2, HCl, NO, H_2, O_2, and Cl_2 for a chamber pressure of 700 kPa, the real oxidizer to fuel ratios, and the corresponding temperatures.

Tab. 2 Calculated oxidizer to fuel ratios, combustion temperatures at 700 kPa, and mass fractions.

Ammonium Perchlorate to Ammonium Nitrate Ratio	**1:1**	**1:1.5**	**1:2**
Oxidizer to Fuel ratio			
Stoichiometric oxidizer to fuel ratio	12.1	12.7	13.2
Real oxidizer to fuel ratio	7.5	7.4	7.3
Combustion temperature			
Chamber temperature (°C) with stoichiometric combustion	2189	2123	2076
Chamber temperature (°C) with real combustion	1892	1747	1643
Propellant mass fractions			
Mass fraction (%) of oxygen in propellant	56.7	57.3	57.7
Mass fraction (%) of free oxygen in propellant	17.6	15.6	14.2
Mass fraction (%) of chlorine in propellant	18.0	14.8	12.7
Exhaust mass fractions			
Mass fraction (%) of H_2 in exhaust gases	11.0	12.9	14.3
Mass fraction (%) of H_2O in exhaust gases	44.1	43.3	42.6
Mass fraction (%) of CO in exhaust gases	10.9	11.1	11.1
Mass fraction (%) of CO_2 in exhaust gases	8.4	7.9	7.7
Mass fraction (%) of N_2 in exhaust gases	15.4	16.5	17.3
Mass fraction (%) of HCl in exhaust gases	10.2	8.2	6.9

Tab. 2 reflects the fact that, under ‘real’ conditions, the mechanical requirements dictate the presence of a stiff outer section to the propellant rod. This means that the oxidizer to fuel ratio is not optimized, and indeed the real oxidizer to fuel ratio is around half of the stoichiometric ratio. This lack of oxidizer produces a temperature lower than the theoretical value and a number of incomplete combustion products, such as H_2 and CO.

We note that, if the mechanical issues attending to the propellant rod stiffness were to be overcome, stoichiometric combustion would yield higher chamber pressures while permitting a greater fraction of AN to be introduced. This would further help to extend the life of the engine.

Alternatively, higher chamber pressures could be obtained with the existing fuel system by using different oxidizers, such as the perchlorates of potassium ($KClO_4$), sodium ($NaClO_4$), or lithium ($LiClO_4$). These substances have greater specific mass than AP and AN, at around 2.5 g/cm^3, so it is possible to place more mass in the same volume. They also decompose into harmless salts and oxygen at heating. The former two perchlorates are reasonable to use for laboratory testing, while the latter seems best for spacecraft applications.

III. Results

A. Experimental data

The results of two consecutive firings are presented in Figs. 4 and 5, except for brief deletions due to excessive noise likely associated with spark plug operation. The force applied to the solid propellant, the resultant propellant rod use, the chamber pressure, and the stagnation temperature near the chamber wall are presented. Please note that, in each figure, the plot on the right is simply a zoomed version of the plot on the left, except that the propellant use is time differentiated (and filtered) to yield a more meaningful propellant consumption rate.

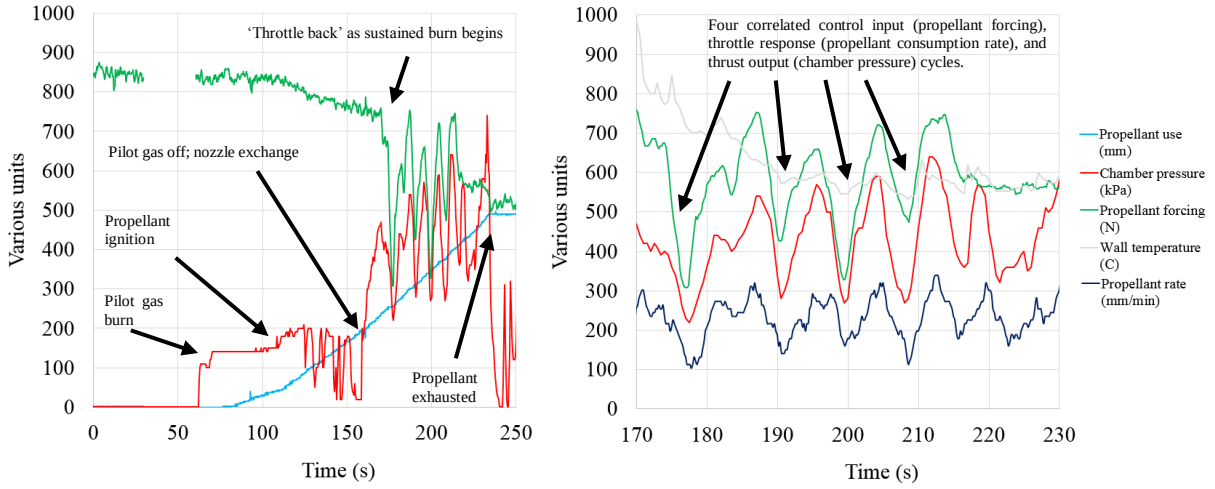

Fig. 4 First firing. The combustion appeared to falter between 125s and 150s.

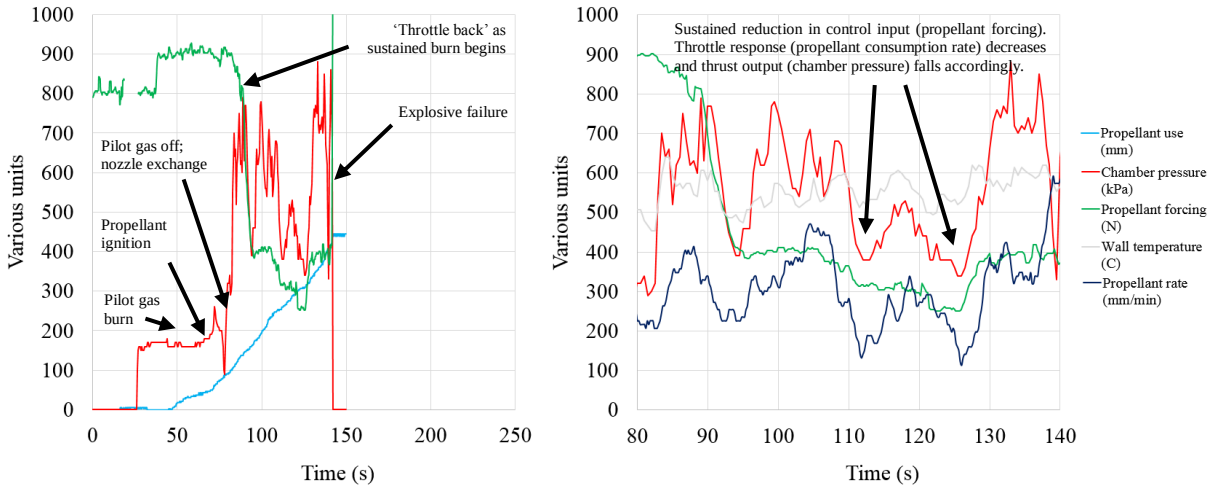

Fig. 5 Second firing. The engine was extinguished by an explosion at 142s.

B. Discussion of the results

In both tests, a number of common features are apparent. Firstly, as the pilot gases are ignited by the spark plug, chamber pressure climbs to about 150 kPa. After around 20s, movement is detected on the propellant rod. This suggests that the vaporizer has been sufficiently heated for propellant vaporization to begin, and we can assume that the gaseous fuel and oxidizer begin to move along their respective channels to the ring of injector ports.

After a few tens of seconds, chamber pressure rises to around 200 kPa. This is associated with blue highlights in the otherwise yellow propane flame, and is considered to be consistent with the ignition of the solid propellant mixture.

The pilot gases are then switched off, but to prevent a loss in pressure the nozzle throat diameter is stepped down from 4 mm to 1.6 mm using the pushrod-operated nozzle exchange system. This appears in the data as a dip in chamber pressure (as the pilot gases are closed) followed seconds later by a surge (as the nozzle is constricted). During this process the operators 'throttle back' the engine by reducing the pressure of the argon supplied to the pneumatic ram which forces the solid propellant rod into the vaporizer. At this stage (around 170s in the first firing, and around 80s in the second firing) the autophage engine has become self-sustaining: the heat of burning propellant gases drives the vaporization of incoming solid propellant as chamber pressures of 400 kPa to 500 kPa are attained.

With the engine running, the two experiments diverge. In the first firing, the 'throttle setting' is cycled four times, between around 300N to 750N of applied force. The objective is to determine if the engine can be throttled up and down, and there is a strong correlation between the throttling cycles and both propellant consumption (which cycles between approximately 100 mm/min and 300 mm/min) and chamber pressure (which cycles between around 300 kPa to almost 700 kPa). During the second firing, however, the force applied to the propellant is gradually reduced to levels as low as 250N while the engine continues to burn.

In both runs, a stagnation temperature of around 550°C is recorded by a thermocouple placed in a gas flow at a distance of 1-2 mm above the combustion chamber inner surface. Some correlation with the throttling cycles is observed, but we note that the steel combustion chamber has considerable thermal inertia which will limit the temperature fluctuations and may also explain the surprisingly low temperature value recorded.

Finally, the first firing concludes as the propellant is exhausted, although there are some final surges before the engine is fully extinguished with nitrogen from the pilot gas manifold. The second firing ends abruptly with an explosion inside the vaporizer that extinguishes the engine and breaks some pressure seals, but which does not rupture the engine itself. Again, the chamber is purged with nitrogen after this event.

C. Opportunities for development

The goal of our work is a lightweight autophage engine suitable for small rocket applications. However, for effective propulsion the chamber pressure should reach the order of 1000 kPa, while the propellant feed pressure should be less, perhaps around 100 kPa, to ensure that the mass of the system is kept as low as possible.

The propellant feed pressure may be estimated by considering the propellant feed force, subtracting a value to account for friction forces between the propellant rod and the vaporizer assembly, and then dividing the force by the area of the propellant rod. Given that a separate experimental investigation has indicated that approximately 125 N is required to insert a propellant rod into a heated vaporizer assembly, Fig. 6 may be obtained. This directly compares the first and second firings and presents the propellant rate and chamber pressure, exactly as before, for reference.

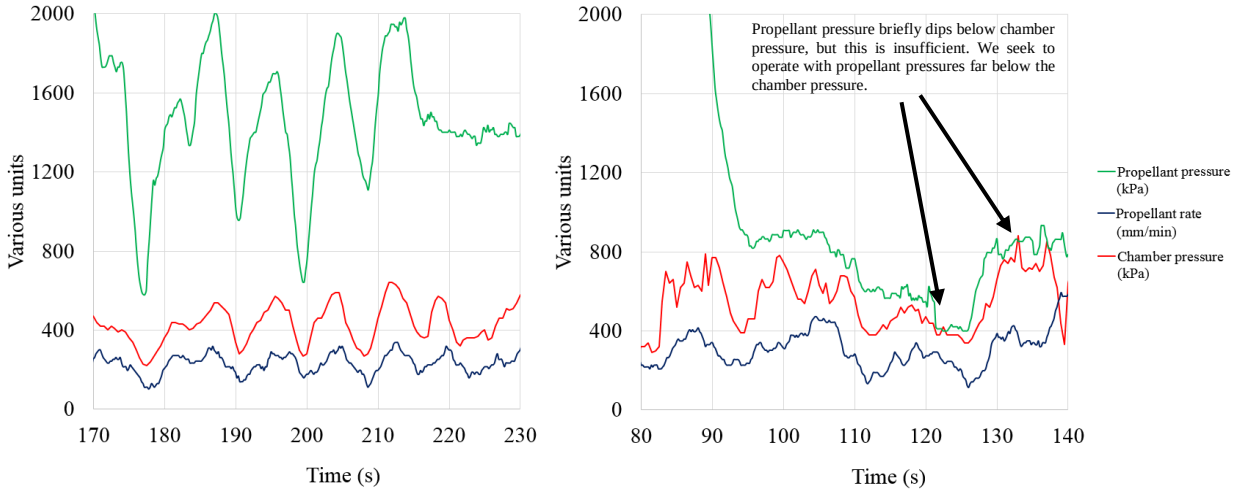

Fig. 6 First firing (left) and second firing (right), with propellant forcing converted to propellant pressure.

This comparison exercise clearly shows the relatively large propellant pressures used to achieve throttling in the first run, contrasted to the low propellant pressures used in the second run. Surprisingly, however, the second run maintained a slightly higher propellant feed rate and, correspondingly, a slightly higher chamber pressure throughout.

No great significance should be read into discrepancies between the two individual tests. The experiments were carried out on two different days, using two different batches of propellant. Small changes in chemistry could have had a marked effect on performance, and the second test did ultimately end in failure.

However, even during the second run, the propellant pressure did remain generally in excess of the combustion chamber pressure. This is not ideal, as we would prefer to operate with propellant pressure far below chamber pressure.

In order to ensure that propellant could continue to flow into the chamber against this adverse pressure gradient, we seek to achieve a pulsed-mode combustion in the chamber. This is why we place flap valves over the injection ports, so that they may admit propellant between pulses, but prevent the products of combustion from flowing back into the vaporizer during the pulse itself. However, the experimental data indicates that the conditions required to initiate pulsed-mode operations (namely, approximately equal pressures on both sides of the flap valves) were not maintained for a reasonable time and there is no evidence that pulsation was achieved. Future work will seek to constrict the nozzle throat still further in order to achieve these conditions and move towards pulsed-mode operations.

D. Characterization of small combustion instabilities

There are some additional oscillations in propellant feed rate, and hence chamber pressure. We consider that a negative feedback loop with respect to the vaporizer and combustion chamber may be at work, whereby high chamber activity promotes vaporization, accelerating propellant feed until the influx of cold propellant slows vaporization and chamber activity falls. However, as the cold propellant then heats up, vaporization begins again and the cycle repeats.

Frequency analysis of the propellant consumption rate (in mm/min) from 170s and 80s, respectively for the first and second runs, until 51s later in both cases (256 data points at the 5 Hz experimental sampling rate), has been carried out using a Hann window and a Fast Fourier Transform, followed by conversion to a power spectral density. The result, shown in Fig. 7, indicates that this dynamic behavior has a period of around 2.9s.

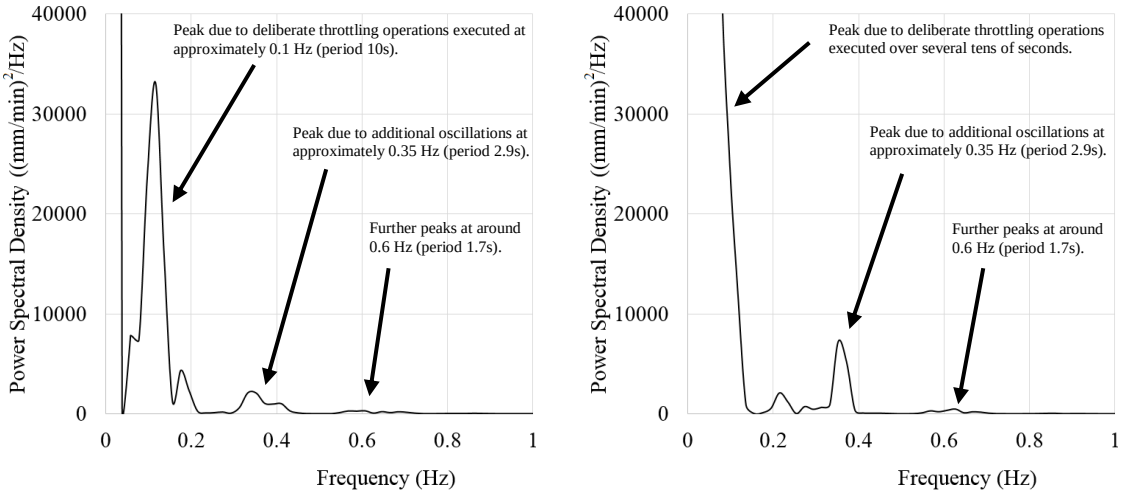

Fig. 7 Propellant consumption rate during the first firing (left) and second firing (right), in frequency domain.

IV. Operational Difficulties

A. Explosive failures

The second firing ended with an explosion, and this has been a repeated problem with the engine. Further technical development is clearly required, perhaps allied with additional work on the ideal propellant chemistry.

Fig. 8 (left) shows the result of a major explosive failure, which destroyed the vaporizer cover and exposed the underlying fuel and oxidizer channels in the vaporizer cone itself. The remains of the tantalum flap valves which used to cover the injector ports are also visible, as is some black fuel residue. The combustion chamber was undamaged.

Fig. 8 (centre) shows the engine disassembled after the smaller explosion, in the same place as before, which extinguished the second run described in this paper. The ends of the flap valves appear to have melted and may have partially blocked the inlet ports, leading to the event that forced the vaporizer cover back off the vaporizer itself. Although some locating pins were sheared, the vaporizer cover was not damaged on this occasion.

Fig. 8 (right), on the other hand, shows an engine core disassembled after a successful firing, with the flap valves removed such that the fuel and oxidizer ports are clearly visible. The presence of brown ash on alternating ports only suggests that the fuel/oxidizer separation system can work very well, with the two constituents being delivered separately and only mixing in the combustion chamber. This figure also shows the copper washer and the pilot gas manifold, with its six inlets: two each for propane, oxygen, and nitrogen.

Nonetheless, the repeated vaporizer events do suggest that explosive conditions can easily develop on the outside of the vaporizer cone. This may be due to insufficient separation of the gases as they are collected from the propellant rod, leakage between adjacent fuel and oxidizer channels underneath the vaporizer cover, or poor flow conditions due to failure of the flap valves.

Fig. 9, in three successive stills from the video record taken about 0.03s apart, shows the magnitude of the forces that these events can generate. A tin cover (circled) is installed at the top of the pneumatic ram used to drive the propellant rod, for the purpose of protecting the feed force transducer underneath. The explosion, in the middle frame, drives the ram (as indicated by the tin position) downwards against the propellant forcing cylinder which was, at that moment, developing a force on the order of 400 N. A cloud of exhaust gas, which has forced its way down the sides of the propellant rod delivery tube to provide this force, can also be seen venting around the ram interface. In the final frame, the ram returns to its normal position.

While these events are undesirable, and the development team continue their efforts to prevent them, the energy that is available in the exhaust gases does seem likely to exceed the energy required to meet the propellant feed force requirements. Therefore, if the valves can be made to operate as intended, and the unwanted explosive behavior eliminated, it is possible that the engine will be able to generate its own feed force in the future. This would further simplify its application.

Fig. 8 Engines disassembled after burns which ended in failure (left and middle) and fuel exhaustion (right).

Fig. 9 An explosive failure. Forced deflection of the ram and force transducer cover (circled) may be seen.

B. Leakage around the nozzle exchange system

When the pilot gases are switched off, it is necessary to reduce the size of the nozzle throat to maintain pressure. This is achieved by sliding a graphite throat block from one position (with a 4mm hole) to another (with a 1.6mm hole) using the nozzle exchange pushrod lever, which passes through the wall and into the operations room.

The sealing between the throat block and another graphite block at the outlet of the combustion chamber is maintained through a contact pressure applied by four coil springs, as shown in Fig. 2. The preload must be high enough to prevent excessive leakage, low enough to allow free movement of the throat block, and stable enough to be maintained even when the springs are exposed to the radiated heat of the exhaust plume. However, the radial patterning in Fig. 10 (left) does indicate that leakage is an ongoing problem when the smaller throat is selected during the high pressure, self-sustaining part of the run.

C. Incomplete combustion

Soot covering the combustion chamber outlet and the nozzle block, as in Fig. 10 (left), is evidence of incomplete burning. This is associated with low temperatures and pressures inside the combustion chamber. The problem is likely insufficient atomization and mixture of the gasiform fuel and oxidizer before combustion.

Additionally, although the solid propellant usually self-sustains combustion after the pilot gases are turned off, the spark plug can be used for re-ignition in the event of a flame-out. On yet another unsatisfactory run, as shown in Fig. 10 (right), the effect of the spark plug positioning can be seen in that there is a build-up of soot on the ‘cold’ side of the chamber. Such incomplete combustion may also partially explain the surprisingly low temperatures observed during some experiments, because the spark plug is located directly opposite the thermocouple.

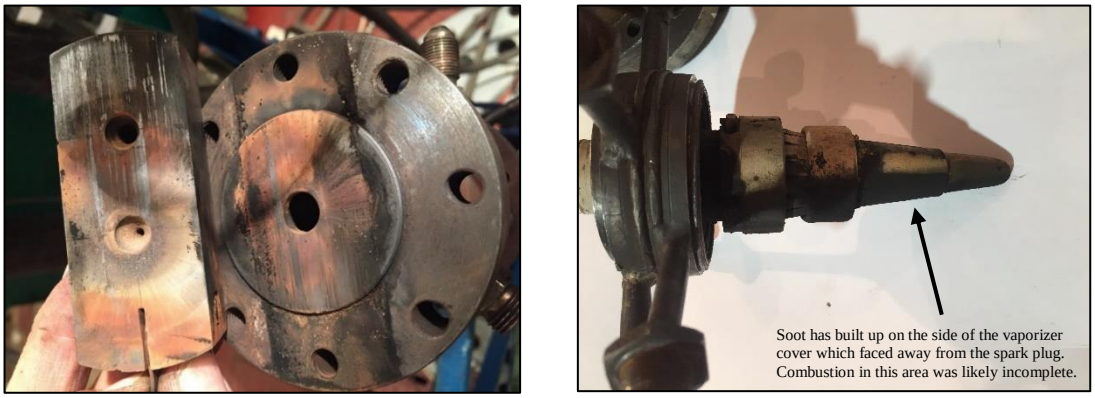

Fig. 10 Disassembled nozzles (left) show leakage, and disassembled engines show uneven burning (right).

V. Advanced Analysis and Next Objectives

An examination of the data from the first firing suggests that it is possible to build a solid propellant rocket engine that can be throttled on demand. The second firing, on the other hand, is an attempt to operate with a very low propellant driving forces. It is our objective to improve the combustion performance such that propellant feed pressure and chamber pressure become approximately equal, because at this point the valves may induce the engine to operate in a state of pulsed combustion by exploiting a resonance in the chamber itself, such that the propellant feed forces may be reduced. Naturally, we wish to predict the frequency at which this behavior may be observed.

Simulations of the combustion with Star CCM (using the non-premixed Eddy Break Up model) are therefore presented. The model is 2D axisymmetric with a timestep of 0.0001s in implicit unsteady time discretization, with a final polyhedral mesh of base size 1×10^{-4} m proving mesh independence and residual error convergence to lower than 1×10^{-5}, with adequate resolution. A 2nd order coupled implicit flow solver was implemented with ideal gas constraints and 1st order κ-ε turbulence, RANS and high Y+ wall treatment solvers. The flap valves are omitted and the thermochemistry is simplified for a less computationally strenuous model: a two-step hydrocarbon decomposition reaction, involving the oxidation of key species via separated mass flow inlets, is used to produce incomplete and complete combustion. Convective boundaries are applied to the chamber walls based on experiment ambient values and, assuming a propellant feed rate of 225 mm/min with 100% AN oxidizer at an oxidizer to fuel ratio of 8.8, the pressure and gas velocity results are as presented in Fig. 11. Full details of the model are provided elsewhere [16].

Due to simplifications to oxidation stoichiometry the simulated chamber pressure and temperature levels obtained, whilst of similar order to test data values, do involve some offsets in range and maxima from theory. The chamber pressure and velocity also showed more significant pulse behavior than did the temperature variations. However, the study of potential internal pulse-wave patterns is a more focused objective than exhaustive thermodynamic validation, and is instead conducted in order to bound the possibilities of natural pulsed combustion as development continues.

It is therefore apparent from Fig. 11 that, on startup, a chugging behavior on the order of 50 Hz may be expected, although it appears to be a transient phenomenon that immediately follows the ignition phase and gives way to a steady-state phase over the course of the next few tenths of a second. The final stabilization pressure is not inconsistent with the experimental data, but the experimental gas velocities are unknown and cannot be compared. In these figures, the silhouette represents a cross-section of one half of the combustion chamber, with the injection ports to the left and the nozzle to the right.

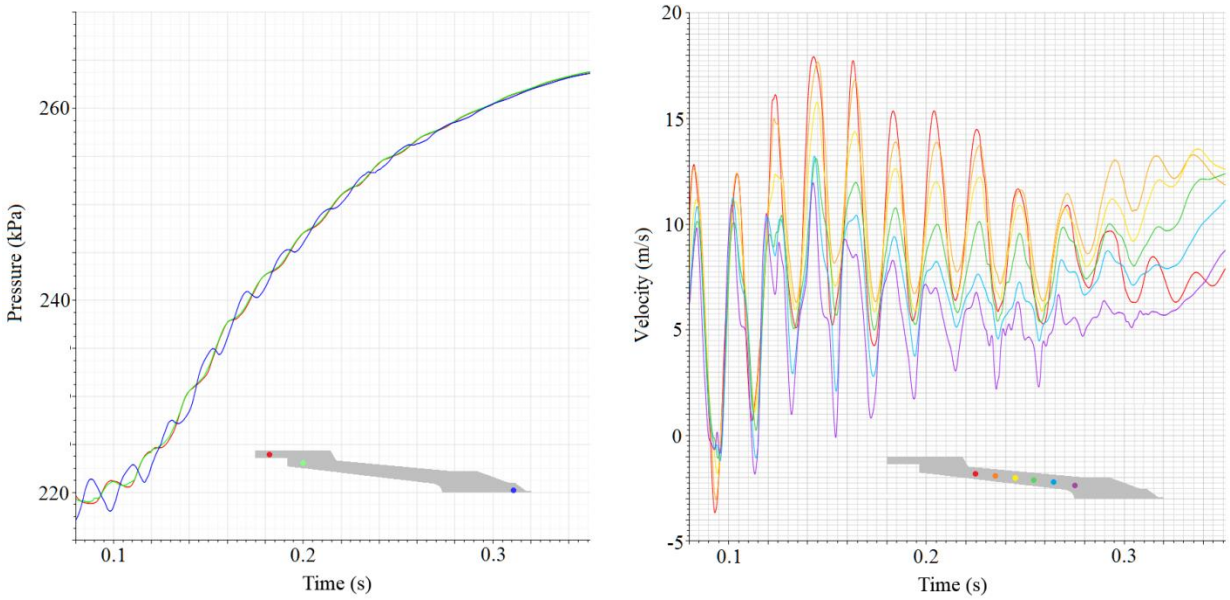

Fig. 11 Simulation of the engine in Star CCM. A transient standing wave (left) with a superimposed velocity behavior (right) is observed. Time is post-ignition.

As previously noted, if pulsed combustion can be achieved by exploiting this behavior, the propellant feed force need only exceed the chamber pressure during its minimum cycle to deliver fuel and oxidizer. This may further reduce the magnitude of the forcing required to feed the solid propellant into the engine, and hence advance the miniaturization of the device mechanics because it may be possible to develop a lighter propellant delivery mechanism. This mechanism may even be powered by the products of combustion themselves, which would allow the engine to feed its own propellant in an 'automatic' manner.

The development team is therefore working on a number of challenges: we seek to correct the faults which can lead to leakage and explosion; to improve the physical and chemical properties of the propellant; to increase the combustion chamber pressure; to eliminate the pilot gases in favor of an electrical start/restart system; to create the circumstances in which the effects of pulsed combustion might be observed; and to explore the possibility of creating an automatic propellant feeding system to exploit those pulsations, powered by bleed gases from the exhaust itself.

VI. Conclusion

An autophage rocket engine, consuming only solid propellant, has been fired in a sustained manner with multiple 'throttle up' and 'throttle down' maneuvers, where chamber pressure was observed to vary with the feed force applied to the solid propellant. The engine requires pre-heating from pilot gases, but once ignited it quickly becomes self-sustaining and the pilot gases may be switched off. An external pneumatic ram is also required to force the propellant rod into the engine at the desired feed rate.

Work has been carried out to reduce the force needed to drive the feed system, and sustained combustion has been achieved with force levels as low as 250N. However, it has been proposed that a resonance inside the chamber may be exploited to reduce this force requirement still further. This resonance is predicted to lie at around 50 Hz.

Finally, several operational difficulties have been identified which can lead to failure or reduced pressure in the combustion chamber. These issues are being addressed by the development team.

Funding Sources

This work has received institutional support from the University of Glasgow and Dnipro National University, in the context of a Collaboration Agreement between our two institutions.

Acknowledgments

The authors thank the technical staff of the Physical and Technical Faculty, and in particular Mr. Oleg Kostritsyn.

References

[1] "Launch Services Program, Program Level Dispenser, and CubeSat Requirements Document." NASA LSP-REQ-317.01. NASA, 2014.

[2] Larson, W. J., and Wertz, J. R. "Space mission analysis and design." Springer, New York, 1991.

[3] Damblane, L. "Self-propelling projectile." U.S. Patent No. 2,114,214. 12 Apr. 1938.

[4] Typaldos, Z. A. "Autophage rocket." U.S. Patent No. 3,250,216. 10 May 1966.

[5] Rhoades, R. G. "Apparatus for staged combustion in air augmented rockets." U.S. Patent No. 4,063,415. 20 Dec. 1977.

[6] Corbett, M. J., and Belisle, J. A. "Single stage autophage rocket." U.S. Patent No. 4,703,694. 3 Nov. 1987.

[7] Isakari, S., Onizuka, S., Yano, Y., and Kakami, A. "Performance evaluation of a throttleable solid propellant thruster using laser heating." *Transactions of the Japan Society for Aeronautical and Space Sciences*, Vol. 14 (30th ISTS), 2016.

[8] Petersen, E., Seal, S., Stephens, M, Reid, D., Carro, R., Sammet, T., and Lepage, A. "Solid propellant rocket motor having self-extinguishing propellant grain and systems therefrom." U.S. Patent No. 8,336,287. 25 Dec. 2012.

[9] Carlson, R. "Method and system for controlling solid propellant thrust." U.S. Patent No. 8,584,443. Nov. 19, 2013.

[10] Yemets, V. V., Dron', M. M., and Yemets, T. V. "An extremely small autophage rocket for orbiting a pico satellite." *Вісник двигунобудування*, Vol. 1, 2015.

[11] Yemets, V. V., Prince, S., and Wilkinson, R. "Investigation of a Combustible Inertial Launch Vehicle Design." *Journal of the British Interplanetary Society*, Vol. 68, 2015.

[12] Yemets, V. V., Dron', M. M., Yemets, T. V., and Kostritsyn, O. "The Infinite Staging Rocket – A Progress to Realization." *66th International Astronautical Congress*, Jerusalem, 12-16 October, 2015.

[13] Лебедев, Б. В. "Термодинамика полиолефинов." *Успехи химии*, Vol. 65, 1996.
[Title Translation: Thermodynamics of polyolefins]

[14] "Химическая энциклопедия." Советская энциклопедия, Большая Российская энциклопедия. Москва, 1988-1999.
[Title Translation: Chemical encyclopaedia]

[15] "Уплотнения и уплотнительная техника." Справочник, Машиностроение, Москва, 1986.
[Title Translation: Seals and sealing technology]

[16] Middleton, M. "Autophage Rocket Design". MSc Thesis, University of Glasgow, 2017.